

Photon waiting-time distributions: A keyhole into dissipative quantum chaos

Cite as: Chaos **30**, 023107 (2020); <https://doi.org/10.1063/1.5127936>

Submitted: 14 September 2019 . Accepted: 14 January 2020 . Published Online: 03 February 2020

I. I. Yusipov, O. S. Vershinina, S. V. Denisov, and M. V. Ivanchenko




[View Online](#)



[Export Citation](#)



[CrossMark](#)

Scilight Highlights of the best new research in the **physical sciences** 

[LEARN MORE!](#)



Photon waiting-time distributions: A keyhole into dissipative quantum chaos

Cite as: Chaos 30, 023107 (2020); doi: 10.1063/1.5127936

Submitted: 14 September 2019 · Accepted: 14 January 2020 ·

Published Online: 3 February 2020



View Online



Export Citation



CrossMark

I. I. Yusipov,¹ O. S. Vershinina,¹ S. V. Denisov,^{2,3} and M. V. Ivanchenko^{1,3,a)}

AFFILIATIONS

¹Department of Applied Mathematics, Lobachevsky University, 603950 Nizhny Novgorod, Russia

²Department of Computer Science, Oslo Metropolitan University, N-0130 Oslo, Norway

³Max Planck Institute for the Physics of Complex Systems, 01187 Dresden, Germany

^{a)}Author to whom correspondence should be addressed: ivanchenko.mv@gmail.com

ABSTRACT

Open quantum systems can exhibit complex states, for which classification and quantification are still not well resolved. The Kerr-nonlinear cavity, periodically modulated in time by coherent pumping of the intracavity photonic mode, is one of the examples. Unraveling the corresponding Markovian master equation into an ensemble of quantum trajectories and employing the recently proposed calculation of quantum Lyapunov exponents [I. I. Yusipov *et al.*, Chaos 29, 063130 (2019)], we identify “chaotic” and “regular” regimes there. In particular, we show that chaotic regimes manifest an intermediate power-law asymptotics in the distribution of photon waiting times. This distribution can be retrieved by monitoring photon emission with a single-photon detector so that chaotic and regular states can be discriminated without disturbing the intracavity dynamics.

Published under license by AIP Publishing. <https://doi.org/10.1063/1.5127936>

Quantification of regimes emerging in open quantum systems driven out of equilibrium is a problem, which is interesting in several respects. In particular, it could help bridging nonequilibrium quantum phenomena with manifestations of classical dissipative chaos, such as local instability, bifurcations, strange attractors, etc.¹ Considerable effort was devoted to quantum generalization of Lyapunov exponents (LEs), the most popular and powerful means to quantify classical chaos.^{2–4} Recently, a new wave of research in this direction has been initiated by the idea of out-of-time correlation functions as possible quantum LE analogs.^{5,7,8} In our recent work,⁹ we proposed yet another approach to “quantization” of LEs, based on unraveling of the Markovian master equation that describes the evolution of the system’s density matrix into an ensemble of trajectories. However, all the approaches suffer from a common problem: while it is possible to define the corresponding observables and correlators and then treat them analytically or calculate numerically, it is much harder (or not possible at all) to access them in a real-life experiment. Here, we demonstrate that “chaos-regularity” transitions can be captured by looking at the statistics of dissipative jump events that are accessible in quantum optics and called these “distribution of photon waiting times.”^{10,11} Exemplifying in a simple model of an open periodically modulated

quantum system, we show that transitions from regular to chaotic regimes (beforehand defined in terms of LEs) are marked by transitions from exponential waiting-time distributions to those with intermediate power-law scaling. Since photon emission events can be resolved in an experiment, e.g., by using single-photon detectors, discrimination between chaotic and regular regimes can, therefore, be achieved without disturbance of the system dynamics.

INTRODUCTION

Recent progress in the fields of experimental quantum physics, such as cavity quantum electrodynamics,¹² cavity optomechanics,¹³ artificial atoms,¹⁴ and polaritonic devices,¹⁵ has given the theory of open quantum systems¹⁶ a new impetus. Different from the typical single-particle models of quantum optics,¹⁰ such systems are essentially multicomponent and thus require many-body models to describe them.

These models, when considered out of equilibrium, display asymptotic states that are sometimes interpreted as quantum versions of chaotic (or regular) attractors.¹ Until recently, such classification was performed mostly visually, after projecting quantum

states onto a suitable classical phase space.^{17–22} The quantitative approach to *dissipative* Quantum Chaos²³ is possible by means of quantum versions of Lyapunov exponents (LEs).²⁴ There is no unique definition of quantum LEs; instead, there are several alternative generalizations ranging from early attempts to define the exponents in terms of quasiclassical distributions^{2–4} to stochastic Schrödinger equation,^{25–30} and further on to a very recent approach based on the concept of out-of-time-correlators.^{5–8} However, all these generalizations suffer a common problem: the corresponding quantifiers are hard (or not possible at all) to measure in a real-life experiment.

In our recent work,⁹ we introduced a version of quantum LEs based on the so-called “quantum trajectory” unraveling^{43,44} [also called the “Monte Carlo wave function (MCwf) method”^{41,42}], which replaces the original quantum Markovian master equation¹⁶ with an ensemble of quantum trajectories. The evolution of the trajectories is governed by a non-Hermitian Hamiltonian in a continuous-time manner, interrupted by random jumplike dissipative events. While this version, in principle, opens a way to theoretical characterization of quantum dissipative chaos in physically relevant setups (e.g., in cavity quantum electrodynamic systems¹²), the experimental estimation of such quantum LEs is no less challenging than for the prior versions.

Here, we propose an experimentally feasible approach to detect chaotic regimes in cavitylike open quantum systems. Namely, using a periodically modulated Kerr-nonlinear cavity as a model, we demonstrate that the transition to quantum chaos, quantified with the LEs from Ref. 9, is associated with the appearance of an intermediate power-law asymptotics in the distribution of waiting time (that is, the time between two consequent photon emissions from the cavity^{32–34}). This distribution can be sampled in an experiment by using single-photon detection techniques.^{35,36}

MODEL

We consider a photonic mode in a leaky Kerr-nonlinear cavity, periodically modulated by an external coherent EM field.^{17,18} Its unitary dynamics is governed by the Hamiltonian (we set $\hbar = 1$),

$$H(t) = \frac{1}{2}\chi\hat{a}^{\dagger 2}\hat{a}^2 + iF(t)(\hat{a}^\dagger - \hat{a}). \quad (1)$$

Here, χ is the photon interaction strength, \hat{a}^\dagger and \hat{a} are photon creation and annihilation operators so that $\hat{n} = \hat{a}^\dagger\hat{a}$ is the photon number operator. $F(t) = F(t + T)$ describes periodic modulation. We use the two-valued quenclike driving with period T , that is, $F(t) = A$ within $0 < t \leq T/2$ and $F(t) = 0$ for the second half period $T/2 < t \leq T$.

Photons can be emitted from the cavity. In principle, they can also be pumped in by thermal environment, but here, similar to the setups in Refs. 17 and 18, we work in the zero-temperature limit, assuming that the pumping rate is zero. Evolution of the cavity is described by the Lindblad master equation^{16,37,38}

$$\dot{\rho} = \mathcal{L}(\rho) = -i[H, \rho] + \mathcal{D}(\rho), \quad (2)$$

where the first term in the r.h.s. captures the unitary dynamics of the system, determined by Hamiltonian (1), while the second term reflects coupling to the environment. The dissipative term involves

a single jump operator,

$$\mathcal{D}(\rho) = V\rho V^\dagger - \frac{1}{2}\{V^\dagger V, \rho\}, \quad V = \sqrt{\gamma}\hat{a}, \quad (3)$$

which describes emission of photons by the cavity into the zero-temperature environment. The dissipative coupling constant γ is assumed to be time-independent.

In simulations, we limit the number of photons in the cavity mode to N so that the Hilbert space of the numerical model has dimension $N + 1$ and can be spanned with the $N + 1$ Fock basis vectors, $\{|n + 1\rangle\}$, $n = 0, \dots, N$. N is chosen to be large enough so that the average number of photons in the cavity, $\langle N_{\text{ph}} \rangle$, remains substantially smaller. $\langle N_{\text{ph}} \rangle$ depends on parameters of Hamiltonian; yet the main control parameter, which allows to control the mean number of photons, is the coupling χ .^{17,18} Throughout the paper, we set $\chi = 0.008$ and $\gamma = 0.05$. It gives $\langle N_{\text{ph}} \rangle \sim 50$, so we set $N = 300$ and verify that it suffices.

We make use of the quantum Monte Carlo wave function method to unravel the deterministic equation (2) into an ensemble of quantum trajectories.^{41–44} It allows us to describe evolution of the model system in terms of an ensemble of pure states, $|\psi(t)\rangle$, governed by the effective non-Hermitian Hamiltonian,^{17,18}

$$i\dot{\psi} = H\psi - \frac{i}{2}V^\dagger V\psi. \quad (4)$$

The norm of the wave function decays according to

$$\frac{d}{dt}\|\psi\| = -\psi^*V^\dagger V\psi, \quad (5)$$

until it reaches a threshold η , repeatedly chosen as i.i.d. random number from $[0, 1]$. Then, a random jump is performed, and the wave function norm is reset to $\|\psi(t)\| = 1$. After that the continuous nonunitary evolution, Eq. (4), is resumed until the next quantum jump, etc. For the model given by Eqs. (1) and (3), a quantum jump corresponds to emission of a single photon, which can be recorded by a photodetector.¹⁰

The density matrix sampled from a set of M_r realizations, that originate from an initial pure state $|\psi^{\text{init}}\rangle$ for Eq. (4), as $\rho(t_p; M_r) = \frac{1}{M_r} \sum_{j=1}^{M_r} |\psi_j(t_p)\rangle \langle \psi_j(t_p)|$, converges toward the solution of Eq. (2) at time t_p for the initial density matrix $\rho^{\text{init}} = |\psi^{\text{init}}\rangle \langle \psi^{\text{init}}|$.

Following Refs. 17 and 18, we use the complex valued observable of the non-Hermitian photon annihilation operator as a dynamical “variable”

$$\xi(t) = \langle \psi^\dagger(t) | \hat{a} | \psi(t) \rangle. \quad (6)$$

In the mean-field classical limit, $N_{\text{ph}} \rightarrow \infty$, its evolution is given by

$$\dot{\xi} = -\frac{1}{2}\gamma\xi + F(t) - i\chi|\xi|^2\xi. \quad (7)$$

The state of the mean-field system is described by two phase variables, $\{\text{Re } \xi, \text{Im } \xi\}$. This system is essentially nonlinear and periodically modulated time and, expectedly, exhibits a spectrum of different asymptotic regimes, from various periodic orbits to chaotic attractors. The parameter dependence can be visualized with a bifurcation diagram [Fig. 1(a)] constructed from stroboscopic values, $\xi_k = \xi(t_0 + kT)$, where t_0 is a transient time given to the system

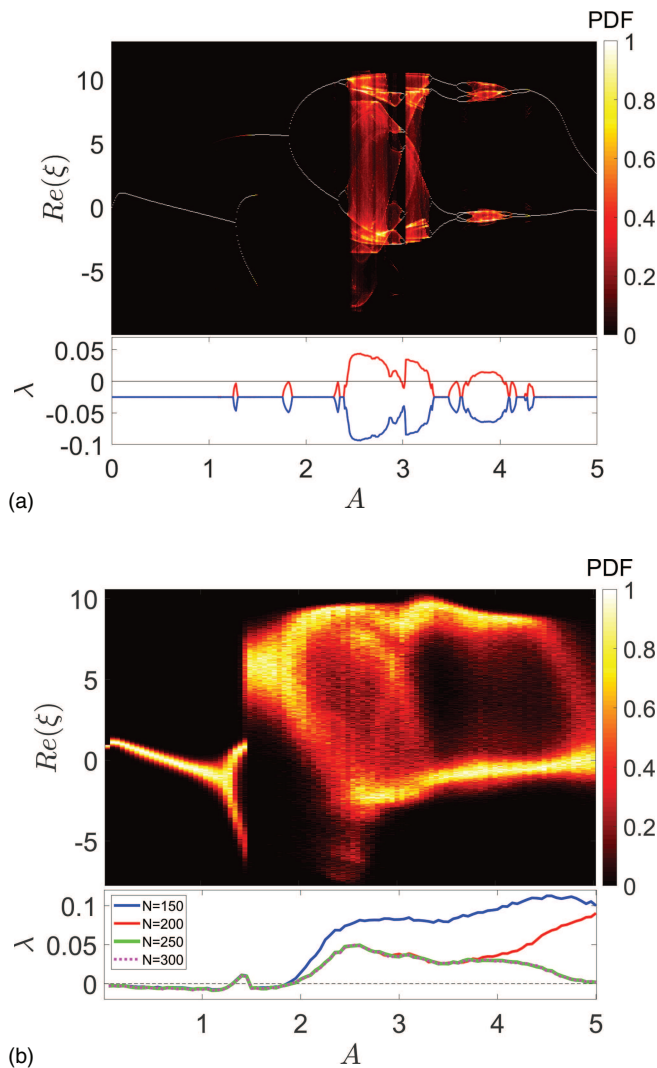


FIG. 1. Bifurcation diagrams and largest Lyapunov exponent for the model system as functions of the modulation amplitude A in the classical (a) and quantum (b) cases. The color-coded probability distributions for $Re(\xi)$ are normalized so that the maximum for every A value is set to 1. The other parameters are $T = 10$, $N = 300$. The values of quantum LE are consistently reproduced, independent of the dimension of the numerical model for $N \geq 250$, (b) bottom panel.

to land on the corresponding attractor. In particular, one observes that the largest Lyapunov exponent becomes positive upon transition from a fixed point to a chaotic attractor in the stroboscopic map [see Fig. 1(b)].

QUANTUM LYAPUNOV EXPONENT

To calculate the largest quantum LE, we employ the recently proposed method.⁹ It is based on the parallel evolution of fiducial and auxiliary trajectories, $\psi_f(t)$ and $\psi_a(t)$, under Eq. (4), in

the spirit of the classical LE calculation.⁴⁵ The auxiliary trajectory is initialized as a normalized perturbed vector $\psi_a^{init} = \psi_f^{init} + \varepsilon \psi_r$, produced with random i.i.d. entries in ψ_r and $\varepsilon \ll 1$. The fiducial and perturbed observables, $\xi_f(t)$ and $\xi_a(t)$, typically remain close to each other over many quantum jump events; as the difference in the observables gets over an upper threshold, $\Delta(t_k) = |\xi_f(t_k) - \xi_a(t_k)| > \Delta_{max}$, or below a bottom threshold $\Delta(t_k) < \Delta_{min}$, the perturbed state is set back closer to the fiducial one along the mismatch direction $\psi_f(t_k) - \psi_a(t_k)$ so that $|\xi_f(t_k) - \xi_a(t_k)| = \Delta_0$; the wave vector gets normalized and the occurred growth rate recorded, $d_k = \Delta(t_k) / \Delta_0$.⁴⁶ The largest LE is estimated following the divergence of the chosen observable as $\lambda(t) = \frac{1}{t} \sum_k \ln d_k$.⁴⁵

We use a recent high-performance realization of the quantum jumps method⁴⁷ to generate $M_r = 10^2$ different trajectories. First, we allow each trajectory to evolve up to $t_0 = 2 \times 10^3 T$ in order to arrive to the asymptotic regime, and then we follow the dynamics of fiducial and auxiliary trajectories up to $t = 10^3 T$. We determine the dimension of the computational model, N , that would be large enough to ensure independence of the results on the chosen value. It has turned out that $N = 150$ is already sufficient for the consistent calculation of the quantum LEs almost in the whole range of modulation amplitude, A [cf. Fig. 1(b), bottom panel]. However, for $A > 3.5$ oscillations of the number of photons in the cavity grow and this leads to the distortion of the dynamics and positive LEs. Ultimately, we find it out that choosing the maximal number of photons $N > 250$ provides consistency in the whole range of studied parameters.

Additionally, we verified convergence of the maximal LE to its asymptotic values in the regular and chaotic regimes and confirm that the results are weakly dependent on the choice of observables [e.g., we used photon population number, $n(t) = \langle \psi^\dagger(t) | \hat{n} | \psi(t) \rangle$, as an alternative] (see Fig. 2).

Depending on parameter values, interaction with the environment can strongly localize quantum trajectories on the classical ones.^{17,18,26,27} Our case is notably different so that the resulting structure of the probability distribution for ξ has only a qualitative resemblance [see Fig. 1(b), top]. Nevertheless, working in the essentially quantum regime, we observe that the largest quantum LE becomes positive [see Fig. 1(b)]. Note that the chaotic interval in the quantum case is somewhat greater, and fine structure intervals of classical regular dynamics are not reproduced. Such examples, when quantization generates chaotic dynamics, are known in the literature.²⁷

To get a more general picture, we performed an extensive round of calculations and obtained the two-parameter dependence of classical and quantum largest LEs on the amplitude and period of modulations [see Figs. 3(a) and 3(b)]. Both the mean-field and quantum models produce visually similar structures of regular and chaotic regimes.

WAITING-TIME DISTRIBUTION

As we pointed it out in the Introduction, quantum LEs are good objects for theoretical and numerical analysis, but their experimental estimation is highly nontrivial.

Can we infer information about intracavity dynamics from what is accessible in experiment? Statistics of fluorescent photon

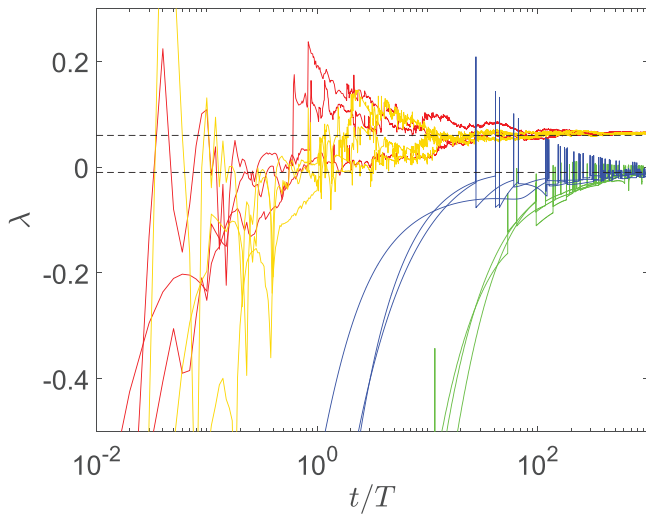


FIG. 2. Convergence of finite time LEs to their asymptotic values, $\lambda = 0$ (regular dynamics) and $\lambda \approx 0.08$ (chaotic regime). Three individual trajectories are used in each case. Exponents are calculated by using, first, $\xi(t)$ as an observable, $A = 0.05, T = 0.5$ (blue), $A = 4.0, T = 20$ (red) and second, the mean number of photons in the cavity, $n(t)$, $A = 0.05, T = 0.5$ (green), $A = 4.0, T = 20$ (orange). Here, $N = 300$.

emission from cavity is one of the most popular characteristics in quantum optics and appears promising for our purpose.^{33,49–51} The other reason for the choice is that there is only one dissipative channel in our model system, and a single quantum jump corresponds

to a single photon emission so that the intracavity dynamics and radiation are tightly bound.

Evolution of the wave vector norm between consecutive quantum jumps at times $\{t_k\}$ is governed by Eq. (5). For the system under study, Eqs. (1) and (3), it follows:

$$\frac{d}{dt} \|\psi\| = -\gamma n(t) \|\psi\|, \tag{8}$$

as $V^\dagger V = \gamma \hat{n}$. The norm decay from $\|\psi(t_{k-1})\| = 1$ to the random jump threshold $\|\psi(t_k)\| = \eta_k$ can be approximated by an exponent with an average rate proportional to an effective number of photons within $t_{k-1} < t < t_k$, that is, $s_k = \gamma n_k^{(eff)}$. In other words, one can write $\tau_k = t_k - t_{k-1} = -\ln(\eta_k)/s_k$. Since η_k are random i.i.d. numbers on $[0, 1]$, the variable $\zeta = -\ln(\eta_k)$ has the probability density distribution $W_\zeta(\zeta) = \exp(-\zeta)$. If an asymptotic density matrix ρ has a regular structure (e.g., unity matrix or unimodal distribution), then $n \approx \text{const}$ and, hence, $s \approx \text{const}$. In this case, the intervals between jumps also follow Poisson distribution, $W_\tau(\tau) = \exp(-\tau)$. Another example is a bimodal asymptotic solution, a result of the quantum analog of period doubling bifurcation,^{20,21} also a regular one, that would produce a superposition of two exponents.

When the system has a chaotic attractor, the dynamics of observables, in particular, $n(t)$, becomes irregular. An example for a quantum trajectory deep in the chaotic regime, $A = 4.0, T = 20$, is presented in Fig. 4(a). It is seen that the norm decay rates between each jump differ substantially. Therefore, the probability distribution $W_\zeta(s)$ cannot be deduced from simple arguments any longer. At the same time, it can be estimated numerically [see Fig. 4(b), upper panel]. The results indicate that the distribution becomes much broader for $A > 0.4$, with transition to chaos [Fig. 4(b), lower panel]. Correspondingly, the resulting distribution of interjump intervals,

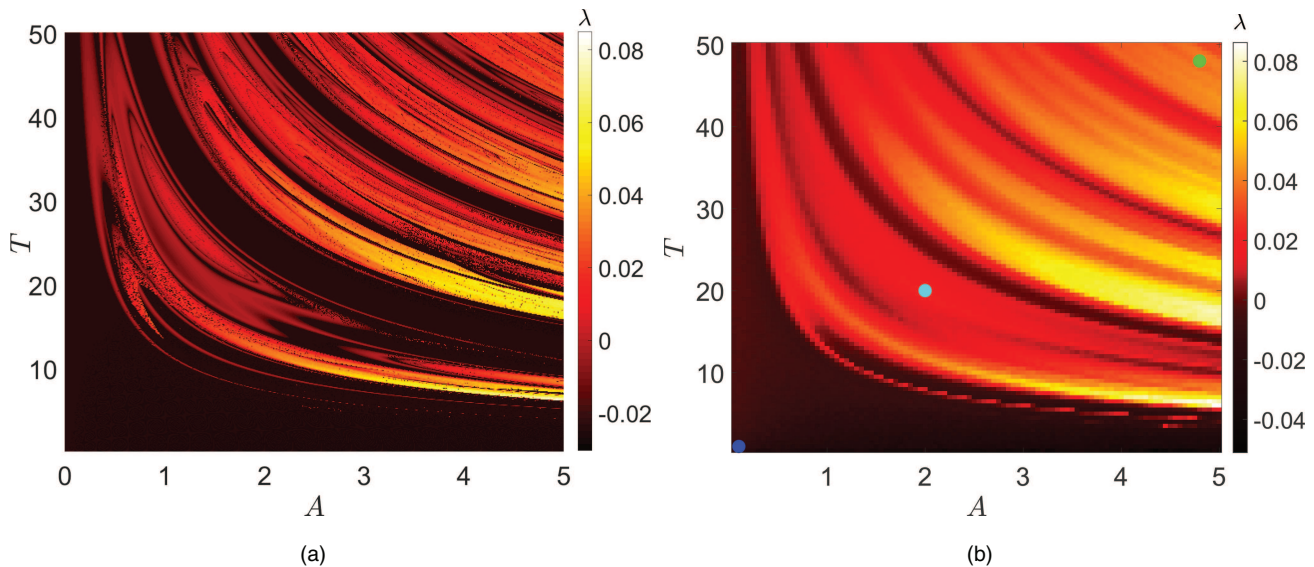


FIG. 3. Largest Lyapunov exponent as a function of amplitude A and period T of the modulations for the model system in (a) the mean-field and (b) quantum versions [selected points correspond to those in Fig. 5(b)]. Here, $N = 300$.

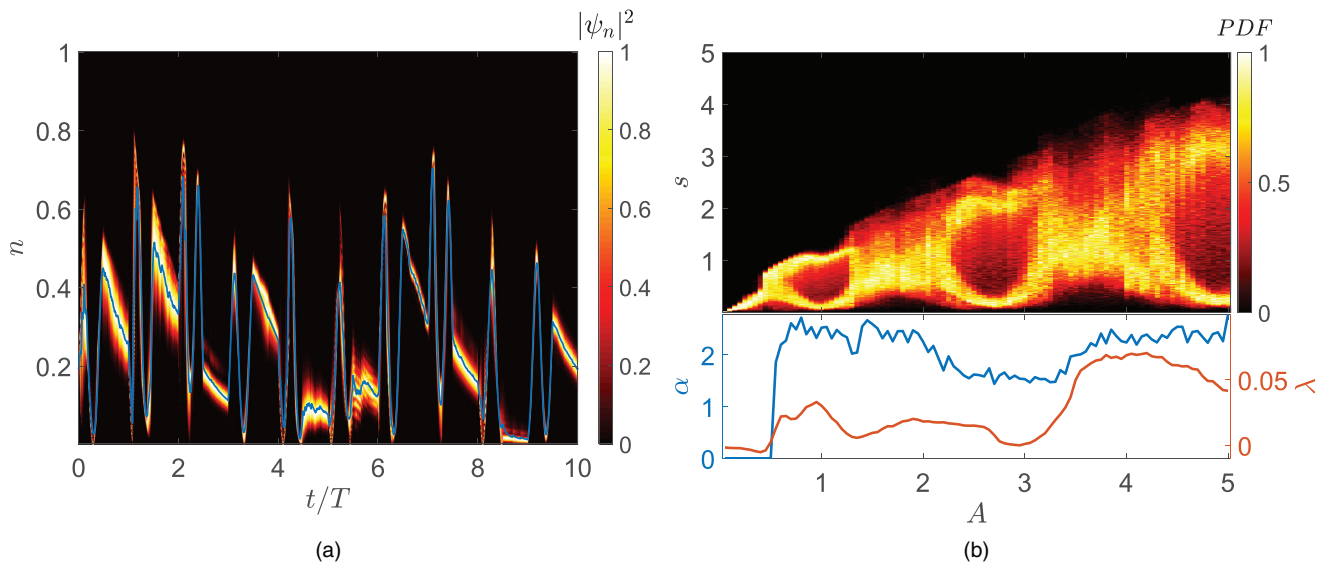


FIG. 4. (a) Wave function evolution for an individual quantum trajectory deep in the chaotic regime for $A = 4.0$, $T = 20$ (color) and expectation $n(t)$ (blue line). (b) PDF of average norm decay rates, $W_s(s)$, between quantum jumps (top). Corresponding largest quantum LE (red) and an exponent for the power-law fit of $W_\tau(\tau)$ (blue, where valid). Note simultaneous broadening of $W_s(s)$, transition to $\lambda > 0$, and appearance of the power-law interval in the time between quantum jumps distribution. Here, $N = 300$.

$W_\tau(\tau)$, will no longer be exponential. In the complete absence of a theoretical background in this case, we turn to numerical simulations.

Our main finding is presented in Fig. 5. The key observation is that the waiting-time distribution becomes non-Poissonian and

acquires a power-law intermediate scaling when the largest quantum LE becomes positive [Fig. 5, see also Fig. 4(b), lower panel].

We performed massive sampling over the parameter plane $\{A, T\}$. At every parameter point, the power-law fitting of the sampled Probability Distribution Function (PDF) was obtained by

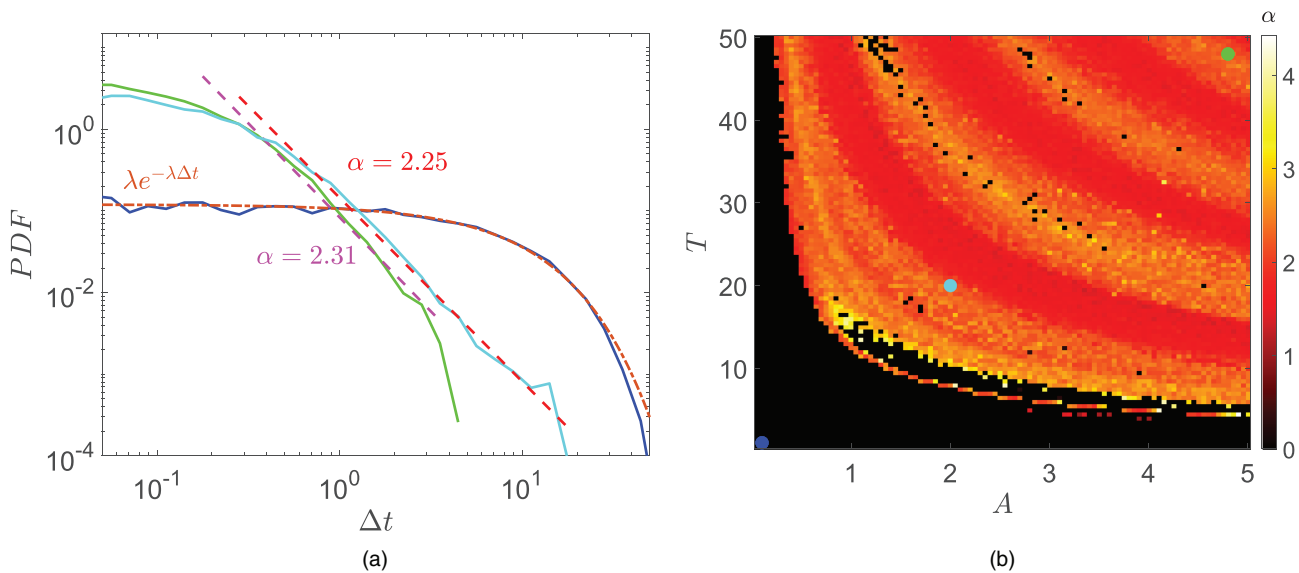


FIG. 5. (a) PDF of time intervals between quantum jumps for selected parameter values, $A = 0.1$, $T = 1$ (blue), $A = 2.0$, $T = 20$ (cyan), and $A = 4.8$, $T = 48$ (green), cf. color matched points in Figs. 3(b) and 5(b), power-law and exponential fits. (b) The heat map for the power-law exponent on the amplitude-period of modulation parameter plane; black color indicates its failure [compare to the largest LE diagram, Fig. 3(b)]. Here, $N = 300$.

the least squares linear regression for the log–log scaled distributions. The quality of fit was characterized by the coefficient of determination,³¹ $R^2 \in [0, 1]$, with larger values corresponding to better fit. We vary the interval of durations to search for the best fit, the power-law exponent α , and request that it spans over at least one decade for the horizontal axis and has $R^2 > 0.98$.⁴⁸ Otherwise, the power-law hypothesis is rejected [black zones in Fig. 5(b)].

It is noteworthy that the zones, where power-law asymptotics in the waiting-time distribution is present, are well correlated with the zones, where the corresponding maximal quantum LE is positive [cf. Fig. 3(b)]. Moreover, there are concordant variations of the values of power-law exponents and of the largest LE.

CONCLUSIONS

By using an open ac-driven Kerr cavity as a model, we found that the photon waiting-time statistics can serve as a good diagnostic tool to detect dissipative quantum chaos by the appearance of power-law intermediate asymptotics (which can be alternatively characterized by the positive largest quantum LE). The theoretical foundation of this observation remains a challenge. We conjecture that the first step would be to assume the statistical independence of the consecutive times t_{j-1}, t_j, t_{j+1} (which is not guaranteed though) and then to implement the machinery used by Scherr and Montroll to derive power-law statistics of photocurrent in amorphous materials.³⁹ Implementation of this program is the subject of future study.

Our results open a new perspective for quantification of regimes emerging in open quantum systems far from equilibrium, especially in such fields as quantum electrodynamics, quantum optics, and polaritonic devices, where photon emission statistics is an established and conventional tool.^{33,49–51} Recently, substantial progress in a nondemolition detection of individual emitted microwave photons has been achieved (see, e.g., Ref. 40) so that the field of microwave quantum optics represents the most appealing opportunity to explore dissipative quantum chaos by waiting-time statistics.

Potential links to self-organized criticality^{52,53} and Lévy flights (recently used to model power-law flip statistics of open spin systems⁵⁴) are other issues worth considering.

ACKNOWLEDGMENTS

The authors acknowledge support of Basis Foundation (Grant No. 17-12-279-1) and the President of Russian Federation (Grant No. MD-6653.2018.2). Numerical simulations were carried out at the Lobachevsky University and Moscow State University supercomputers. Work performed in parts and supported by the MPI-PKS Advanced Study Group: Open quantum systems far from equilibrium.

REFERENCES

- ¹E. Ott, *Chaos in Dynamical Systems*, 2nd ed. (Cambridge University Press, 2002).
- ²M. Toda and K. Ikeda, *Phys. Lett. A* **124**, 165 (1987).
- ³F. Haake, H. Wiedemann, and K. Zyczkowski, *Ann. Phys.* **1**, 531 (1992).
- ⁴V. I. Man'ko and R. Vilela Mendes, *Physica D* **145**, 330 (2000).

- ⁵E. B. Rozenbaum, S. Ganeshan, and V. Galitski, *Phys. Rev. Lett.* **118**, 086801 (2017).
- ⁶A. Bohrdt, C. B. Mendl, M. Endres, and M. Knap, *New J. Phys.* **19**, 063001 (2017).
- ⁷Y. Liao and V. Galitski, *Phys. Rev. B* **98**, 205124 (2018).
- ⁸J. Chavez-Carlos *et al.*, *Phys. Rev. Lett.* **122**, 024101 (2019).
- ⁹I. Yusipov, O. S. Vershinina, S. V. Denisov, S. P. Kuznetsov, and M. V. Ivanchenko, *Chaos* **29**, 063130 (2019).
- ¹⁰H. Carmichael, *An Open Systems Approach to Quantum Optics* (Springer, Berlin, 1993).
- ¹¹F. Brange, P. Menczel, and C. Flindt, *Phys. Rev. B* **99**, 085418 (2019).
- ¹²H. Walther, B. T. H. Varcoe, B.-G. Englert, and Th. Becker, *Rep. Prog. Phys.* **69**, 1325 (2006).
- ¹³M. Aspelmeyer, T. J. Kippenberg, and F. Marquardt, *Rev. Mod. Phys.* **86**, 1391 (2014).
- ¹⁴J. Q. You and F. Nori, *Nature* **474**, 589 (2011).
- ¹⁵T. Feurer, J. C. Vaughan, and K. A. Nelson, *Science* **299**, 374 (2003).
- ¹⁶H.-P. Breuer and F. Petruccione, *The Theory of Open Quantum Systems* (Oxford University Press, Oxford, 2002).
- ¹⁷T. P. Spiller and J. F. Ralph, *Phys. Lett. A* **194**, 235 (1994).
- ¹⁸T. A. Brun, I. C. Percival, and R. Schack, *J. Phys. A Math. Gen.* **29**, 2077 (1996).
- ¹⁹M. Hartmann, D. Poletti, M. Ivanchenko, S. Denisov, and P. Hänggi, *New J. Phys.* **19**, 083011 (2017).
- ²⁰M. V. Ivanchenko, E. A. Kozinov, V. D. Volokitin, A. V. Liniov, I. B. Meyerov, and S. V. Denisov, *Ann. Phys.* **529**, 1600402 (2017).
- ²¹G. G. Carlo, L. Ermann, A. M. F. Rivas, M. E. Spina, and D. Poletti, *Phys. Rev. E* **95**, 062202 (2017).
- ²²I. I. Yusipov and M. V. Ivanchenko, *Sci. Rep.* **9**, 17932 (2019).
- ²³F. Haake, *Quantum Signatures of Chaos*, 3rd ed. (Springer-Verlag, Berlin, 2010).
- ²⁴A. Pikovsky and A. Politi, *Lyapunov Exponents: A Tool to Explore Complex Dynamics* (Cambridge University Press, 2016).
- ²⁵N. Gisin and I. C. Percival, *J. Phys. A Math. Gen.* **25**, 5677 (1992).
- ²⁶T. Bhattacharya, S. Habib, and K. Jacobs, *Phys. Rev. Lett.* **85**, 4852 (2000).
- ²⁷B. Pokharel, M. Z. R. Misplon, W. Lynn, P. Duggins, K. Hallman, D. Anderson, A. Kapulkin, and A. K. Pattanayak, *Sci. Rep.* **8**, 2108 (2018).
- ²⁸A. Kapulkin and A. Pattanayak, *Phys. Rev. Lett.* **101**, 074101 (2008).
- ²⁹J. Finn, K. Jacobs, and B. Sundaram, *Phys. Rev. Lett.* **102**, 119401 (2009).
- ³⁰K. Kingsbury, C. Amey, A. Kapulkin, and A. Pattanayak, *Phys. Rev. Lett.* **102**, 119402 (2009).
- ³¹N. R. Draper and H. Smith, *Applied Regression Analysis*, Wiley Series in Probability and Statistics (Wiley, New York, 1998).
- ³²R. Vyas and S. Singh, *Phys. Rev. A* **40**, 5147 (1989).
- ³³H. J. Carmichael, S. Singh, R. Vyas, and P. R. Rice, *Phys. Rev. A* **39**, 1200 (1989).
- ³⁴X. H. H. Zhang and H. U. Baranger, *Phys. Rev. A* **97**, 023813 (2018).
- ³⁵A. Delteil *et al.*, *Phys. Rev. Lett.* **112**, 116802 (2014).
- ³⁶J. D. Cohen *et al.*, *Nature* **520**, 522 (2015).
- ³⁷G. Lindblad, *Commun. Math. Phys.* **48**, 119 (1976).
- ³⁸R. Alicki and K. Lendi, *Quantum Dynamical Semigroups and Applications*, Lecture Notes in Physics Vol. 286 (Springer, Berlin, 1987).
- ³⁹H. Scher and E. Montroll, *Phys. Rev. B* **12**, 2455 (1975).
- ⁴⁰J.-C. Besse, S. Gasparinetti, M. C. Collodo, T. Walter, P. Kurpiers, M. Pechal, Ch. Eichler, and A. Wallraff, *Phys. Rev. X* **8**, 021003 (2018).
- ⁴¹R. Dum, A. S. Parkins, P. Zoller, and C. W. Gardiner, *Phys. Rev. A* **46**, 4382 (1992).
- ⁴²K. Mølmer, Y. Castin, and J. Dalibard, *J. Opt. Soc. Am. B* **10**, 524 (1993).
- ⁴³M. B. Plenio and P. L. Knight, *Rev. Mod. Phys.* **70**, 101 (1998).
- ⁴⁴A. J. Daley, *Adv. Phys.* **63**, 77 (2014).
- ⁴⁵G. Benettin, L. Galgani, and J.-M. Strelcyn, *Phys. Rev. A* **14**, 2338 (1976).
- ⁴⁶Alternatively, one can make renormalization at regular intervals.⁴⁵ LE converges essentially to the same value, provided that the closeness of trajectories is ensured.⁹
- ⁴⁷V. Volokitin, A. Liniov, I. Meyerov, M. Hartmann, M. Ivanchenko, P. Hänggi, and S. Denisov, *Phys. Rev. E* **96**, 053313 (2017).

⁴⁸We find that taking more or less stringent conditions for the validity of the power law fit can make a difference in “marginal” zones, where the largest LE is next to zero, and quantum chaos is weak or absent. These zones correspond to periodic windows in the classical system bifurcation diagram. However, the main border between regularity and chaos is identified robustly.

⁴⁹A. Delteil, W. Gao, P. Fallahi, J. Miguel-Sanchez, and A. Imamoğlu, *Phys. Rev. Lett.* **112**, 116802 (2014).

⁵⁰R. Sáez-Blázquez, J. Feist, F. J. García-Vidal, and A. I. Fernández-Domínguez, *Phys. Rev. A* **98**, 013839 (2018).

⁵¹F. Brange, P. Menczel, and C. Flindt, *Phys. Rev. B* **99**, 085418 (2019).

⁵²D. Marković and C. Gros, *Phys. Rep.* **536**, 41 (2014).

⁵³M. A. Muñoz, *Rev. Mod. Phys.* **90**, 031001 (2018).

⁵⁴M. Issler, J. Höller, and A. Imamoğlu, *Phys. Rev. B* **93**, 081414(R) (2016).